Mechanisms of SiO_2 Etching: Ab Initio Calculations on the Reactions of CF_m^- ($m = 3-1$) and NF_n^- ($n = 2, 1$) Ions with Local Surface Models

Arndt Jenichen

Institute of Physical and Theoretical Chemistry, University Leipzig, Permoserstrasse 15, D-04318 Leipzig, Germany

Received: February 5, 1997; In Final Form: April 30, 1997[⊗]

The mechanisms of SiO_2 etching by CF_m^- ($m = 3-1$) and NF_n^- ($n = 2,1$) are investigated by applying quantum chemical ab initio methods on local molecular surface models. From the calculated energetic data of intermediate hypercoordinated centers formed by adsorption of the negatively charged ions, the reaction behavior at the surface is estimated. The CF_m^- and NF_n^- ions act as blockers for Si centers, provide chemisorbed F^- ions, or enable the Si−O bond cleavage. At higher temperatures (energy supply of about 37 kcal/mol), the blocking ions desorb and Si−O bonds break.

1. Introduction

The removal of SiO_2 structures is known from glass etching. However, etching processes are also important steps for the microstructuration of integrated circuits. The most frequently applied technology is dry etching by plasmas. A large number of neutral and charged species is formed within the discharges. Their individual roles for etching are important for the optimization of etching processes but are largely unclear. The essential mechanism is the weakening and breaking of bonds which connect the surface atoms with the substrate by reactive species. However, the surface can also be blocked by chemisorbed species.

For the etching of Si/SiO_2 systems, fluorocarbon and fluoronitrogen discharges are preferentially employed.[1,2] Experiments demonstrated that the products of a discharge in NF_3 etch Si and SiO_2 1−2 orders of magnitude faster than those of a similar discharge in CF_4. Two reasons were mentioned: A discharge is much more effective at dissociating NF_3 than CF_4 due to the lower bond strengths of NF_3. No polymerization forming surface-blocking films is found for NF_3, contrary to pure fluorocarbon plasmas.[3,4]

In some previous papers,[5,6] the Si−O bond breaking by neutral CF_m ($m = 4-1$) and NF_n ($n = 3-1$) was theoretically investigated. The main result that CF_2 is the most efficient molecule for SiO_2 etching is in accordance with LASER experiments.[7] The reliability of the used quantum chemical method was demonstrated for the systems HF + Si[8−10] and HF/HCl + SiO_2.[11]

Theoretical investigations to the reactions of CF_m^+ ($m = 3-1$) and NF_n^+ ($n = 2-1$)[12] showed that at low temperature the SiO_2 surface can be blocked by CF_3^+ and CF_2^+. Chemisorbed CF^+, NF_2^+, and NF^+ allow the breaking of Si−OSi bonds by cyclic rearrangements. At higher temperatures as in discharges all the ions favor the breaking of Si−OSi and Si−OH bonds.

Silicon atoms can form bonds with more than four atoms simultaneously.[13] The most stable molecules with hypercoordinated Si are negatively charged.[13−19] Stishovite is an example for hypercoordination in SiO_2 solids.[20] Six-coordinated silicon atoms were also found in glasses.[21] Therefore, hypercoordinated Si atoms could also be expected as intermediates during reactions of negatively charged ions with SiO_2 surfaces.

In this paper, the reactions of CF_m^- ($m = 1-3$) and NF_n^- ($n = 1, 2$) as well as F^- ions at the SiO_2 surface structures are investigated. Various bonds formed between the ions and the saturated Si and O atoms are considered. For stable hypercoordinated structures, possible bond-breaking reactions are investigated. First the used molecular surface models and quantum chemical methods are described. Then the free ions and the deformation processes of the surface structures are investigated. Finally the stability of possible hypercoordinated surface complexes is discussed, and the results are compared with other theoretical data and experimental findings.

2. Models

For the investigation of the reactions at the Si center and at the Si−O bond, three models are applied:

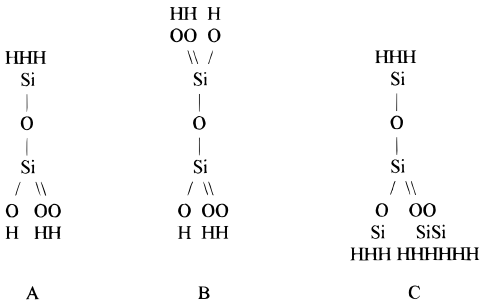

Ab initio calculations require the restriction to relatively small surface cut-outs.[22] The influence of long-range interactions as well as steric constraints must be neglected. Furthermore, the very many surroundings of the reaction centers in a reaction layer, as other reactants, intermediates, and products, cannot be considered by these models. Therefore, the obtained results cannot exactly agree with real surface data. However, they should provide the different reaction behaviors of the various reactive species. The used model sizes should be sufficient for finding of the mechanisms and the most efficient species for Si−O bond breaking by chemical reactions.

Sterical constraints should not be of essential importance, as shown in the following consideration: The formation of five-coordinated Si-centers leads to a change of the location of the attacked Si atom to the neighboring Si atoms. This concerns the distances and the orientation as can be seen from Figure 1. The Si−O−Si bridge angle of SiO_2 (α-quartz) was found to be about 144°.[23] Theoretical investigations on disiloxane show that the potential energy curve for the Si−O−Si angle is very flat.

[⊗] Abstract published in *Advance ACS Abstracts,* June 15, 1997.

S1089-5647(97)00450-1 CCC: $14.00

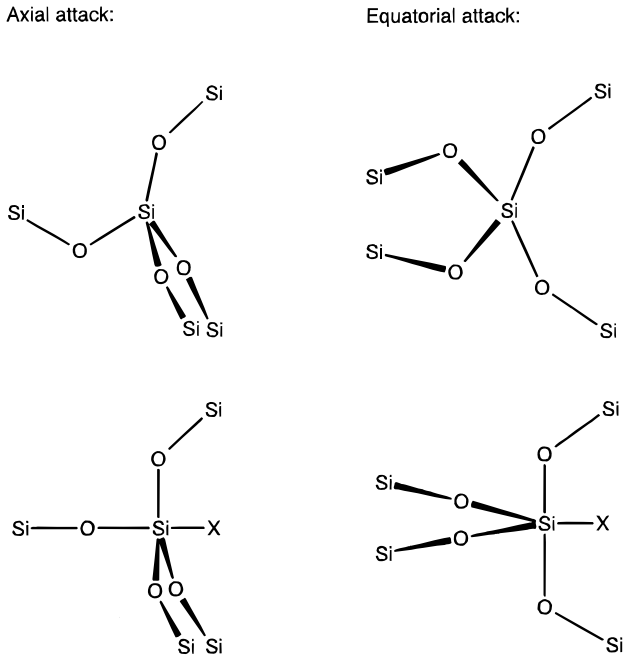

Figure 1. Formation of five-coordinated Si atoms.

The variation between 125° and 180° leads to a maximum energy change of 1−2 kcal/mol.[24, 25] This allows the lengthening and shortening of the Si−Si distances as well as the deformation of the Si−O−Si bridges, which are necessary for the formation of hypercoordinated structures at surfaces, without large energy rise. The deformation energies for the change of coordination at the Si centers are much higher as shown in section 4.2.

3. Methods

The ab initio calculations were carried out with the GAUSSIAN 92 program system.[26] The geometry optimizations and the force constant calculation were done with the restricted and unrestricted Hartree−Fock method and the 3-21G(*) [27] (method I) and, for estimation of the influence of the basis, the 6-31+G* [28−31] (method II) basis set. The gradients and force constants are calculated by analytical methods.[32,33] The zero-point vibrational energies (ZPE) were corrected for known deficiencies of Hartree−Fock calculated frequencies with a scaling factor of 0.89.[34] The energies were obtained using the 6-31+G* (I) and 6-31++G** (II) basis sets and the Møller−Plesset perturbation theory[35] of second order (MP2) with frozen cores. The calculated $\Delta_D H$ are dissociation enthalpies for $T = 0$ K.

4. Results and Discussion

4.1. Ions. Calculations for the lowest spin multiplicities of the free ions show that the singlet (S) and doublet (D) states have the lowest energy. The only exception is CF^-. For this ion a triplet (T) state is more stable. As calculations showed, all the complexes with CF^- also have a triplet ground state. For all other systems the ground state has the lowest spin multiplicity.

The net atomic charges calculated by the Mulliken population analysis are presented for the free ions in Table 1. The charges of the fluorine atoms are nearly equal for all the ions (−0.5e). The carbon atom of CF_3^- has a positive charge (+0.6*e*). C and N of CF_2^- and NF_2^- are approximately neutral. CF^- and NF^- have a negative charge of about −0.45*e* at C and N, respectively.

TABLE 1: Atomic Distances *R* (Å) and Atomic Charges *q* (*e*) (Mulliken Population) of the Free Ions Using Method I

free ion (multiplicity)	*R*(C/N−F)	*q*(C/N)	*q*(F)
CF_3^- (S)	1.438	+0.60	−0.53
CF_2^- (D)	1.469	+0.08	−0.54
CF^- (T)	1.507	−0.44	−0.56
NF_2^- (S)	1.513	−0.08	−0.46
NF^- (D)	1.556	−0.47	−0.53

TABLE 2: Deformation Energies for Formation of Trigonal Bipyramidal Structures with Free Equatorial or Axial Positions Calculated by Method I (kcal/mol)

model	equatorial	axial
A	77.3	53.0
C	81.2	51.9

TABLE 3: $\cdots O_4Si-FAF_{m-1}^-$ Structures with F in Axial Position: Some Atomic Distances *R* (Å) and Dissociation Enthalpies $\Delta_D H$ (kcal/mol) Calculated by Model A and Method I

	$\Delta_D H$ Si−F_{ax}A	*R* Si−F_{ax}A	$\Delta_D H$ SiF−A	*R* SiF−A	*R* AFSi−O_{ax}
CF_3^-	4.8	1.657	3.3 (S)	2.125	1.661
CF_2^-	4.3	1.654	3.8 (D)	2.087	1.659
CF^-	4.1	1.681	12.2 (T)	1.886	1.668
NF_2^-	2.1	1.700	12.8 (S)	1.779	1.668
			−39.0 (T)		
NF^-	2.3	1.680	18.5 (D)	1.808	1.666
			−60.1 (Q)		

The negative charge of the ions (nucleophile) favors the attack on the positively charged silicon atoms of SiO_2. From the charge distribution a preferential orientation of the ions during the attack can be expected. CF_2^- and NF_2^- should preferentially cause a Si−F interaction. For CF_3^-, an O−C and Si−F interaction can be favored.

4.2. Deformation. The formation of hypercoordinated Si atoms of SiO_2 structures is connected with the deformation of the tetrahedral oxygen atom coordination at the Si centers. The ideal five-coordination requires a trigonal-bipyramidal structure. The attack of the negative ions is imaginable on the axial and equatorial position (Figure 1). Table 2 presents the deformation energies for the formation of free axial or equatorial positions. In comparison with the axial position the equatorial one requires about 30 kcal/mol more energy for the rearrangement. The differences between the models A and C are small. As will be shown in the following sections, the formation of the ion−Si bond can yield the deformation energies for the axial and equatorial positions.

4.3. $\cdots O_4Si-F-AF_{m-1}^-$ Structures. Calculations show that the oxygen atoms of the SiO_2 models do not form stable bonds with the considered ions. Therefore, with the exception of the dissocative chemisorption at a Si−O bond, in this paper the interaction of the ions with the Si centers are investigated only. At first the $\cdots O_4Si-FAF_{m-1}^-$ and then the $\cdots O_3FSi-OAF_{m-1}^-$ as well as $\cdots O_4Si-AF_m^-$ surface complexes are discussed (A = C or N).

Tables 3 and 4 present some atomic distances and dissociation enthalpies of structures formed by attack of a F atom of a CF_m^- or NF_n^- ion on a Si atom of the local surface model A.

In the axial position all the ions show a small energetic stabilization by the complex formation ($\Delta_D H$/Si−FA) which increases in the following order:

$$NF_2^- < NF^- < CF^- < CF_2^- < CF_3^-$$

For the equatorial position the same order is found. However, only CF_3^- and CF_2^- lead to a decrease of the energy. The NF^-

TABLE 4: $\cdots O_4Si-FAF_{m-1}^-$ Structures with F in Equatorial Position: Some Atomic Distances *R* (Å) and Dissociation Enthalpies $\Delta_D H$ (kcal/mol) Calculated by Model A and Method I

	$\Delta_D H$ Si−F_{eq}A	*R* Si−F_{eq}A	$\Delta_D H$ SiF−A	*R* SiF−A	*R* FSi−O_{ax}
CF_3^-	5.2	1.643	4.0 (S)	2.207	1.715
CF_2^-	4.5	1.645	4.2 (D)	2.149	1.716
CF^-	−0.3	1.656	8.1 (T)	1.968	1.710
NF_2^-	−3.8	1.665	7.1 (S)	1.866	1.707
			−44.6 (T)		
NF^-		1.615		∞	1.727

ion does not form a stable structure. The F^- binds to Si and the N atom leaves the complex during the optimization.

The small energetic stabilization with the complex formation results, on the one hand, from the weakening of the SiF−C/N bonds. This can be seen from the facts that the Si−F distances are close to lengths of normal Si−F bonds and the SiF−AF_{m-1} distances are strongly increased. On the other hand, the large deformation energy, which is necessary for the attack of the F atom on the Si center (see section 4.2), lowers the energetic stabilization of the complexes.

The last two facts suggest a barrier for the F attack on a Si center. However, this could not be confirmed by the calculations. That means that in the process of complex formation the energy gained in the Si−F binding suffices to yield the energy necessary for the deformation described in section 4.2.

The reaction behavior at the surface can be obtained from the enthalpies of possible dissociation reactions of the complexes where the Si−O bond cleavage, however, is not considered because of the high bond strength (see section 4.5): By reason of the small formation enthalpies of the complexes compared with the SiF−AF_{m-1} dissociation enthalpies, the bound CF_3^- and CF_2^- should preferentially set free CF_2 and CF, respectively. Considering that the triplet (T) state of NF is much more stable than the singlet (S) state and the quartet (Q) state of N is much more stable than the doublet (D) state, NF and N also desorb from the complexes, respectively. However, CF^- should again leave the complex (reverse formation reaction):

$$\cdots O_4Si + AF_m^- \leftrightarrow \cdots O_4Si-F\text{--}AF_{m-1}^- \rightarrow \cdots O_4Si\text{--}F^- + AF_{m-1}$$

As result of the reaction, $\cdots O_4SiF^-$ structures remain at the surface. They are investigated in section 4.5. CF_2, CF, NF, and N are desorbed into the gas phase. CF_2 is a very efficient etchant molecule as found both experimentally[7] and theoretically.[5,6] However, the formed carbon species are also able to polymerize. The polymer layer can block the surface and stop the etching. Therefore, the continuation of etching requires the removal of the formed polymeric overlayer by highly energetic plasmas or ionic beams.

4.4. Dissociative Chemisorption: $\cdots O_4FSi-OAF_{m-1}^-$ Structures. Tables 5 and 6 present some atomic distances as well as dissociation enthalpies for structures formed by cleavage of a F−C/N bond of an ion and formation of a Si−F and a O−C/N bond. For the other imaginable dissociative chemisorption process with Si−C/N and O−F bond formation, stable structures were not found by the calculations.

The energetic stabilization by dissociative chemisorption ($\Delta_D H$/F−SiO−A) increases in the following order:

$$CF_3^- < CF_2^- < CF^- < NF^- < NF_2^-$$

The carbon ions cause a higher energy decrease by F atom attack on the equatorial position than on the axial one. The stabilization increases with decreasing number of fluorine atoms in the ions. The nitrogen ions lead to a stronger stabilization than the carbon ions. The stabilization is higher in the axial position than in the equatorial one and decreases with the number of F atoms. Therefore, the F atoms of the carbon ions should prefer more the equatorial than the axial position, contrary to the nitrogen ions.

The reaction behavior can again be obtained from the enthalpies of possible dissociation reactions of the formed complexes: The cleavage of the Si−F bond is not probable because the Si−F bond strength at five-coordinated Si atoms is the highest one as will be demonstrated in section 4.5. The Si−F bond length is also close to that of a normal Si−F bond.

The O−C/N bond dissociation enthalpies increase in the following order with respect to the desorbing products:

$$CF_2\ (S) < CF\ (D) < C\ (T) < NF\ (S) < N\ (D)$$

Because the triplet state (T) of NF and the quartet state (Q) of N are more stable than the singlet (S) and doublet (D) states, respectively, the complexes belonging to these products are instable. NF and N are desorbed (A = N; m = 2, 1):

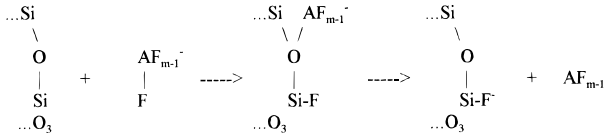

The reactions of the obtained $\cdots O_4SiF^-$ structure are discussed in section 4.5.

The noncharged carbon species CF_2 and CF also desorb very easy (A = C; m = 3, 2). However, the Si−O bond dissociation and the removal of the ions from the complexes (reverse formation reaction) can also play a role because the dissociation enthalpies are not very different. The Si−O bond strengths increase in the following order with respect to the attacking ions:

$$CF_3^- < CF_2^- < CF^- < NF^- < NF_2^-$$

The low Si−O dissociation enthalpies (up to 10 kcal/mol for carbon complexes) are an indication of high etch rates. In addition to the desorption of CF_2 and CF, the following reactions are also probable for the carbon ions:

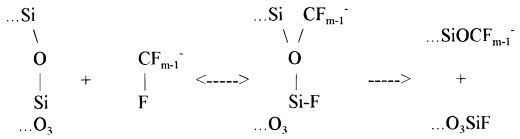

The other Si−O bonds of the obtained surface product structures can be broken by the analogous reactions as discussed.

4.5. $\cdots O_4Si-AF_m^-$ Structures. Tables 7 and 8 present data of the five-coordinated complexes formed by the attack of the carbon or nitrogen atoms of the investigated ions on the Si atoms in axial and equatorial position. Here the F^- ion formed from the ions at the surface (section 4.3. and 4.4.) or in the gas phase (plasma) is also considered.

For the estimation of the influence of larger surface models, calculations were also performed with models B and C. For the calculations with the model C the H_3Si geometry and the Si−O−Si bond angle were fixed in the optimized data of the free model molecule. The comparison of the calculated enthalpies shows that the enlargement of the molecule leads to

TABLE 5: $\cdots O_4FSi-OAF_{m-1}^-$ Structures with F in Axial Position: Some Atomic Distances *R* (Å) and Dissociation Enthalpies $\Delta_D H$ (kcal/mol) Calculated by Model A and Method I

	$\Delta_D H$ $F_{ax}-SiO-A$	*R* $F_{ax}-SiOA$	*R* $SiO_{eq}-A$	$\Delta_D H$ $SiO_{eq}-A$	*R* $FSi-O_{eq}A$	$\Delta_D H$ $FSi-O_{eq}A$
CF_3^-	−1.4	1.603	1.721	2.6 (S)	1.715	−3.7
CF_2^-	5.3	1.605	1.785	5.0 (D)	1.699	4.7
CF^-	7.0	1.604	1.821	15.4 (T)	1.694	5.6
NF_2^-	19.6	1.638	1.596	24.4 (S)	1.728	14.7
				−27.4 (T)		
NF^-	16.1	1.606	1.704	35.1 (D)	1.692	10.7
				−43.5 (Q)		

TABLE 6: $\cdots O_4FSi-OAF_{m-1}^-$ Structures with F in Equatorial Position: Some Atomic Distances *R* (Å) and Dissociation Enthalpies $\Delta_D H$ (kcal/mol) Calculated by Model A and Method I

	$\Delta_D H$ $F_{eq}-SiO-A$	*R* $F_{eq}-SiOA$	*R* $SiO_{ax}-A$	$\Delta_D H$ $SiO_{ax}-A$	*R* $FSi-O_{ax}A$	$\Delta_D H$ $FSi-O_{ax}A$
CF_3^-	5.8	1.599	1.602	4.7 (S)	1.830	3.5
CF_2^-	8.3	1.605	1.721	8.0 (D)	1.802	7.7
CF^-	10.9	1.604	1.775	19.3 (T)	1.788	9.4
NF_2^-	18.2	1.605	1.613	29.0 (S)	1.811	13.4
				−22.8 (T)		
NF^-	12.7	1.603	1.778	31.7 (D)	1.797	7.3
				−46.9 (Q)		

TABLE 7: $\cdots O_4Si-AF_m^-$ Structures with A = C/N in Axial Position: Net Charges *q* (*e*) of the Ions within the Complexes, Some Atomic Distances *R* (Å), and Dissociation Enthalpies $\Delta_D H$ (kcal/mol)

			method I				method II	
		$-q$ ions	$\Delta_D H$ $Si-A_{ax}$	*R* $Si-A_{ax}$	$\Delta_D H$ $Si-O_{ax}$	*R* $Si-O_{ax}$	$\Delta_D H$ $Si-A_{ax}$	$\Delta_D H$ $Si-O_{ax}$
CF_3^-	A	0.61	35.1	1.931	55.3	1.811	38.0	52.9
	C	0.67	27.2	1.951	49.0	1.702		
CF_2^-	A	0.60	30.1	1.920	49.3	1.834	32.6	47.9
	C	0.66	20.3	1.953	44.7	1.711		
CF^-	A	0.56	25.2	1.923	44.3	1.861	27.8	41.8
	C	0.66	14.5	1.987	36.6	1.718		
NF_2^-	A	0.67	30.8	1.897	55.6	1.805	31.7	53.6
	C	0.72	26.0	1.970	52.0	1.695		
NF^-	A	0.57	44.7	1.872	52.5	1.828	46.3	49.3
	C	0.64	36.8	1.910	44.9	1.708		
F^-	A	0.50	53.0	1.624	43.3	1.906	56.3	41.1
	B	0.50	47.4	1.627	40.3	1.879		
	C	0.52	40.0	1.653	36.3	1.732		

a decrease of the Si−F and Si−O bond dissociation enthalpies from model A over model B to model C. The qualitative relations are not influenced by the different models.

The Mulliken population analysis shows that the negative charge of the ions is largely located in the chemisorbed ions (−0.46*e* to −0.72e). The charges of the bound ions increase in the following order:

$$F^- < CF^- < NF^- < CF_2^- < CF_3^- < NF_2^-$$

The largest charge transfer is found for F^- (about 0.50*e* for an axial and 0.54*e* for an equatorial attack). The electronic charge is nearly completely transferred to the dangling bond hydrogen atoms. The enlargement of the model molecules leads to a smaller or an unchanged charge transfer from the chemisorbed ion to the surface model. The attack on axial position causes a smaller charge transfer than the equatorial variant.

An enlargement of the of the basis from method I (MP2/6-31+G*//HF/3−21G(*)) to method II (MP2/6-31++G**//HF/6-31+G*) leads to slightly more stable Si−F bonds (1−3 kcal/mol) and to slightly weaker Si−O bonds (1−3 kcal/mol).

The interaction of the C and N atoms of the ions with the Si centers is the strongest stabilization ($\Delta_D H$/Si−A) found among the studied complexes. It increases in the following order with respect to the ions:

$$\{CF^-, CF_2^-, NF_2^-\} < CF_3^- < NF^- < F^-$$

The largest decrease of the energy is found for an attack of F^- and NF^-. The stabilization by an attack on the axial position is larger than on the equatorial one because of the higher deformation energy in the latter one (see section 4.2).

As well known, the weakest bonds of five-coordinated structures are in the axial position. This is also true for the different Si−O bonds, as confirmed by calculations. The dissociation enthalpies for the axial Si−O bonds increase in the following order for axial and equatorial ion attack:

$$F^- < CF^- < CF_2^- < NF^- < \{CF_3^-, NF_2^-\}$$

Only for the F^- cases the axial Si−O bond is the weakest bond of the complex. Therefore, only the F^- attack should allow the cleavage of a Si−O bond:

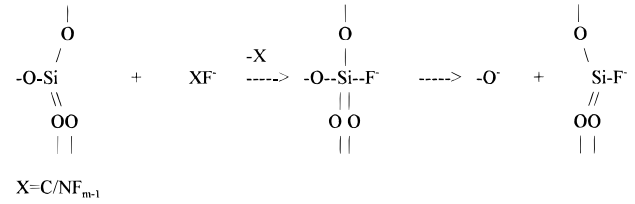

This bond breaking requires a relatively large energy of about 37 kcal/mol (model C) which does not allow a measurable etching at room and lower temperature.

The other ions (C/NF_m^-) are more weakly bound than the oxygen atoms at the Si atoms. Therefore, these ions are blocking the Si centers and can be removed by an energy supply of about 37 kcal/mol (model C) (plasma, ion beam). An experimental support that these ions are not able to remove Si atoms in this positon follows from the fact that no products containing Si−C and Si−N bonds were found. Si atoms are removed as SiF_4.[36]

5. Comparisons

From the interpretation of the data follows that the CF_m^- should be more efficient for etching than the NF_n^- ions: The

TABLE 8: $\cdots O_4Si-AF_m^-$ Structures with A = C/N in Equatorial Position: Net Charges *q* (*e*) of the Ions within the Complexes, Some Atomic Distances *R* (Å), and Dissociation Enthalpies $\Delta_D H$ (kcal/mol)

		method I				
		$-q$ ions	$\Delta_D H$ Si−A_{eq}	*R* Si−A_{eq}	$\Delta_D H$ Si−O_{ax}	*R* Si−O_{ax}
CF_3^-	A	0.56	25.1	1.932	45.3	1.701
	C	0.56	19.7	1.931	41.4	1.717
CF_2^-	A	0.54	23.9	1.903	43.2	1.705
	C	0.56	14.1	1.911	38.5	1.732
CF^-	A	0.52	23.2	1.888	42.2	1.726
	C	0.54	16.4	1.896	38.5	1.730
NF_2^-	A	0.63	20.4	1.895	45.2	1.701
	C	0.63	14.2	1.928	40.2	1.709
NF^-	A	0.54	38.9	1.852	43.7	1.722
	C	0.55	30.7	1.884	38.8	1.721
F^-	A	0.46	46.4	1.615	36.5	1.727
	C	0.46	38.7	1.620	34.2	1.730

desorption of the blocking N-ions requires more energy (up to 37 kcal/mol) than the C-ion desorption (up to 27 kcal/mol). The Si−O bond cleavage by the N-ions goes via $\cdots O_4SiF^-$ complexes (about 37 kcal/mol). For the C-containing ions the Si−O bond breaking after the dissociative chemisorption is more probable because the Si−O dissociation enthalpies are smaller than 10 kcal/mol. Therefore, the lower etch rate of CF_4 discharges, in comparison with NF_3 discharges, must result from another origin.

As shown,[12] the positively charged ions can cause the differences. The NF_n^+ ions allow the breaking of Si−O bonds. CF_3^+ and CF_2^+ ions are blocking the surface. The polymer layer formation by the carbon species and the different properties of the discharges can also be the reasons for the experimental finding.[3,4]

6. Summary

Si atoms are able to have a higher coordination than four, especially for negatively charged systems. The transfer of this fact to reactions of negative ions with SiO_2 structures suggests that hypercoordinated structures occur as intermediates during etching processes. By using local molecular models for SiO_2 surface structures and applying quantum chemical methods, imaginable hypercoordinated adsorption structures formed by CF_m^- ($m = 3-1$) and NF_n^- ($n = 2,1$) ions were investigated with respect to bond weakening and breaking.

The highest energetic stabilization by interaction with the considered ions results from the Si−C/N bond formation. In these structures, the Si−O bonds are not weaker than the Si−C/N bond. Therefore, the ions block the Si centers and must be removed for enabling other surface reactions (about 37 kcal/mol).

The strongest weakening of a Si−O bond, which is the prerequisite for the Si−O bond cleavage as the elementary etching reaction, is obtained by the dissociative chemisorption of a F−C/N bond of an ion at a Si−O bond.The resulting Si−O bond dissociation enthalpies are smaller than 15 kcal/mol. However, this mechanism is restricted to the C-containing ions only.

Not only NF_2^- and NF^- but also CF_3^- and CF_2^- form $\cdots O_4SiF^-$ complexes by desorption of neutral species (NF, N, CF_2, and CF). In these complexes the cleavage of a Si−O bond (about 37 kcal/mol) should be possible for high temperature.

Acknowledgment. Computer time was made available by HLRZ/Forschungszentrum Jülich.

References and Notes

(1) Flamm, D. L.; Donnelly, V. M. *Plasma Chem. Plasma Proc.* **1981**, *1*, 317.
(2) VanRoosmalen, A. J. *Vacuum* **1984**, *34*, 429.
(3) Greenberg, K. E.; Verdeyen, J. T. *J. Appl. Phys.* **1985**, *57*, 1596.
(4) Ianno, N. J.; Greenberg, K. E.; Verdeyen, J. T. *J. Electrochem. Soc.* **1981**, *128*, 2174.
(5) Jenichen, A.; Johansen, H. *Surf. Sci.* **1988**, *203*, 143.
(6) Jenichen, A. *Surf. Sci.* **1995**, *331*, 1503.
(7) Brannon, J. H. *Appl. Phys. A* **1988**, *46*, 39.
(8) Tachibana, A.; Kurosaki, Y.; Kawauchi, S.; Yambe, T. *J. Phys. Chem.* **1991**, *95*, 1716.
(9) Tachibana; A.; Kawauchi, S.; Yambe, T. *J. Phys. Chem.* **1991**, *95*, 2471.
(10) Kawauchi, S.; Tachibana, A.; Yambe, T. *J. Phys. Chem.* **1991**, *95*, 6303.
(11) Jenichen, A. *Int. J. Quantum Chem.* **1994**, *52*, 117.
(12) Jenichen, A. *J. Phys. Chem.* **1996**, *100*, 9820.
(13) Tandura, S. N.; Voronkov, M. G.; Alekseev, N. V. *Topics in Current Chemistry*; Boschke, F. L., Ed.; Springer: Berlin, 1986; Vol. 131, Chapter 3, pp 99−189.
(14) Damrauer, R.; Burggraf, L. W.; Davis, L. P.; Gordon, M. S. *J. Am. Chem. Soc.* **1988**, *110*, 6601.
(15) Holmes, R. R. *Chem. Rev.* **1990**, *90*, 17.
(16) Chuit, C.; Corriu, J. P.; Reye, C.; Young, J. C. *Chem. Rev.* **1993**, *93*, 1371.
(17) Gutsev, G. L. *Chem. Phys.* **1992**, *166*, 57.
(18) Windus, T. L.; Gordon, M. S.; Davis, L. P.; Burggraf, L. W. *J. Am. Chem. Soc.* **1994**, *116*, 3568.
(19) Damrauer, R.; Hankin, J. A. *Chem. Rev.* **1995**, *95*, 1137.
(20) Sinclair, W.; Ringwood, A. E. *Nature* **1978**, *272*, 714.
(21) Dupree, R.; Holland, D.; Mortuza, M. G. *Nature* **1987**, *328*, 416.
(22) Sauer, J. *Chem. Rev.* **1989**, *89*, 199.
(23) Levien, L.; Prewitt, C. T.; Weidner, D. J. *Am. Mineral.* **1980**, *65*, 920.
(24) Nicholas, J. B.; Winans, R. E.; Harrison, R. J.; Iton, L. E.; Curtiss, L. A.; Hopfinger, J. A. *J. Phys. Chem.* **1992**, *96*, 7958.
(25) Csonka, G. I.; Erdösy, M.; Réffy, J. *J. Comput. Chem.* **1994**, *15*, 925.
(26) Frisch, M. J.; Trucks, G. W.; Head-Gordon, M.; Gill, P. M. W.; Wong, M. W.; Foresman, J. B.; Johnson, B. G.; Schlegel, H. B.; Robb, M. A.; Replogle, E. S.; Gomperts, R.; Andres, J. L.; Raghavachari, K.; Binkley, J. S.; Gonzalez, C.; Martin, R. L.; Fox, D. J.; Defrees, D. J.; Baker, J.; Stewart, J. J. P.; Pople, J. A. *GAUSSIAN 92*; Gaussian, Inc.: Pittsburgh, PA, 1992.
(27) Pietro, W. J.; Francl, M. M.; Hehre, W. J.; DeFrees, D. J.; Pople, J. A.; Binkley, J. S. *J. Am. Chem. Soc.* **1982**, *104*, 5039.
(28) Hehre, W. J.; Ditchfield, R.; Pople, J. A. *J. Chem. Phys.* **1972**, *56*, 2257.
(29) Hariharan, P. C.; Pople, J. A. *Theor. Chim. Acta* **1973**, *28*, 213.
(30) Francl, M. M.; Pietro, W. J.; Hehre, W. J.; Binkley, J. S.; Gordon, M. S.; DeFrees D. J.; Pople, J. A. *J. Chem. Phys.* **1982**, *77*, 3654.
(31) Clark, T.; Chandrasekhar, J.; Spitznagel, G. W.; Schleyer, P. v. R. *J. Comput. Chem.* **1983**, *4*, 294.
(32) Pulay, P. *Modern Theoretical Chemistry*; Schaefer, H. F., III, Ed.; Plenum: New York, 1977; Vol. 4, Chapter 4.
(33) Pople, J. A.; Krishnan, R.; Schlegel, H. B.; Binkley, J. S. *Int. J. Quantum Chem. Symp.* **1979**, *13*, 225.
(34) Pople, J. A.; Schlegel, M. B.; Krishnan, R.; DeFrees, D. J.; Binkley, J. S.; Frisch M. J.; Whiteside, R. A. *Int. J. Quantum Chem. Symp.* **1981**, *15*, 269.
(35) Møller, C.; Plesset, M. S. *Phys. Rev.* **1934**, *46*, 618.
(36) vanVeldhuizen, E. M.; Bisschops, T.; vanVliembergen, E. J. W.; vanWolput, J. H. M. C. *J. Vac. Sci. Technol. A* **1985**, *3*, 2205.